PROCEEDINGS, 50th Workshop on Geothermal Reservoir Engineering
Stanford University, Stanford, California, February 10-12, 2025
SGP-TR-229

Exploration for Blind Geothermal Systems in the Eastern Great Basin of Utah: An Update on the "Lund North" INGENIOUS Detailed Study Site

Hardwick, C.L.[1*], Szymanski, E.[1**], Hart-Wagoner, N.R.[2], Ashton, S.[1], Christensen, N.[1], Earney, T.E.[3], Faulds, J.E.[2], Glen, J.M.[3], Hiscock, A.[1], Kirby, S.[1], Knudsen, T.[1], Kobe, S.[1], Lindsey, C.[2], Morbeck, B.L.[3], Peacock, J.[3], Rea-Downing, G.[3], Schermerhorn, W.D.[3], Smith, K.[1]

[1] Utah Geological Survey, 1594 W. North Temple, Suite 3110, Salt Lake City, UT 84116

[2] Great Basin Center for Geothermal Energy, Nevada Bureau of Mines and Geology, University of Nevada, Reno, NV 89557, USA

[3] U.S. Geological Survey, Moffett Field, CA 94035

*christianhardwick@utah.gov,**eugenes@utah.gov

Keywords: INGENIOUS, Great Basin, exploration, hidden, blind, geology, geophysics, geochemistry, lidar

ABSTRACT

Existing geothermal production in Utah is commonly collocated with surficial expressions of geothermal heat including active hot springs and hot spring deposits. However, geothermal potential across the Great Basin region is thought to be much higher for hidden or blind geothermal systems. Accordingly, exploration techniques that can locate geothermal resources that lack surface thermal features could support future development of these systems. The goal of the INGENIOUS project is to reduce exploration risk and discover new, economically viable hidden geothermal systems in the Great Basin region. This paper summarizes the efforts and preliminary results of blind geothermal resource prospecting in Utah as part of the larger INGENIOUS project. The Lund North site in the Basin and Range province of southwest Utah was designated as the fourth detailed study site for the project. The site was initially identified from the preliminary Play Fairway Analysis (PFA) geothermal favorability map, which is based on various data elements, and the identification of favorable structural settings across Utah. This site contains existing legacy data including a thermal gradient borehole with a heat-flow value exceeding 220 mW/m^2. New data collected at this site include terrestrial gravity, magnetotellurics, transient electromagnetics, fluid geochemistry, geologic mapping, UAV-based lidar, paleomagnetism, aeromagnetic surveys, and a shallow temperature survey. Preliminary data and model interpretations corroborate the presence of a large, east-dipping, northeast-southwest-trending normal fault on the edge of a typical Basin and Range graben. Quaternary fault mapping refined by high-resolution lidar surveys suggests a complex step over fault geometry. Utilizing multi-disciplinary datasets for further site assessment at Lund North will facilitate the development of a local-scale PFA and geothermal conceptual model. This new data will be used to site successive thermal gradient drilling to verify heat flow with temperatures at depth at the Lund North site and further investigate the existence of a local geothermal system.

1. INTRODUCTION

The primary goal of the INnovative Geothermal Exploration through Novel Investigations Of Undiscovered Systems (INGENIOUS) project is to accelerate discoveries of new, commercially viable hidden geothermal systems in the Great Basin region (GBR) of the Basin and Range province in the western USA, while substantially reducing the exploration and development risks for all geothermal resources (Ayling et al., 2022). The GBR is a world-class geothermal province with >1,200 MWe of installed nameplate capacity from ~28 geothermal systems. However, studies indicate far greater potential for conventional hydrothermal systems in the region (Williams et al., 2009; U.S. Department of Energy, 2019). The INGENIOUS project integrates Play Fairway Analysis (PFA), three-dimensional (3D) and conceptual modeling, resource capacity estimation, machine learning (ML), advanced geostatistics, and value-of-information (VOI) analysis to identify prospective geothermal resources. Detailed studies of particularly promising sites can provide a means of testing these models and potentially validating refinements in the PFA and associated workflows.

The INGENIOUS team is analyzing four individual sites: 1) northern Granite Springs Valley in western Nevada; 2) northern Reese River Valley (also referred to as Argenta Rise) in north-central Nevada, 3) Jersey Summit/Buffalo Valley, also in north-central Nevada, and 4) Lund North in southwestern Utah (Figure 1). These sites were selected using varying amounts of available information and at different stages of this project. The 4th detailed study site was planned to be in the eastern Great Basin in western Utah to add geographic diversity, considering that all other detailed study sites reside in Nevada, and to increase geologic diversity, as Utah contains areas of relatively high strain rate both within the regional carbonate aquifer and proximal to mafic to felsic Quaternary volcanic fields.

A catalog of two hundred and fifty prospective geothermal leads was developed for Utah's GBR using "favorable structural settings" (FSS) criteria for blind geothermal systems (e.g., Faulds and Hinz, 2015). Regional INGENIOUS datasets were utilized to screen, prioritize, down-select, and then characterize potential sites using key datasets such as the location, recency, slip rates, and slip and dilation tendency of Quaternary faults and the age, composition, and vent locations of Quaternary volcanic deposits. Additionally, the results of the preliminary regional geothermal favorability maps (see Hart-Wagoner et al., 2024) were considered at each potential site.

Twelve sites were identified during this initial screening process, and four were high-graded for more detailed review. These sites are all centered in southwestern Utah due to relatively high strain rates, structural complexity, and proximity to Quaternary volcanic fields,

among other factors. Field reconnaissance of these sites was conducted to verify locations of Quaternary faults, review the existing geologic mapping, acquire new drone imagery, and sample springs where possible. The "Lund North" lead was selected as the 4th INGENIOUS detailed study site for reasons that include (1) favorable geology, (2) the local potential for geothermal, (3) favorable groundwater considerations, (4) the likely positive impact of new technical data to reduce geologic risk uncertainty at the site, and (5) site access and land ownership considerations. The existence of previously acquired detailed aeromagnetic data also factored in this selection.

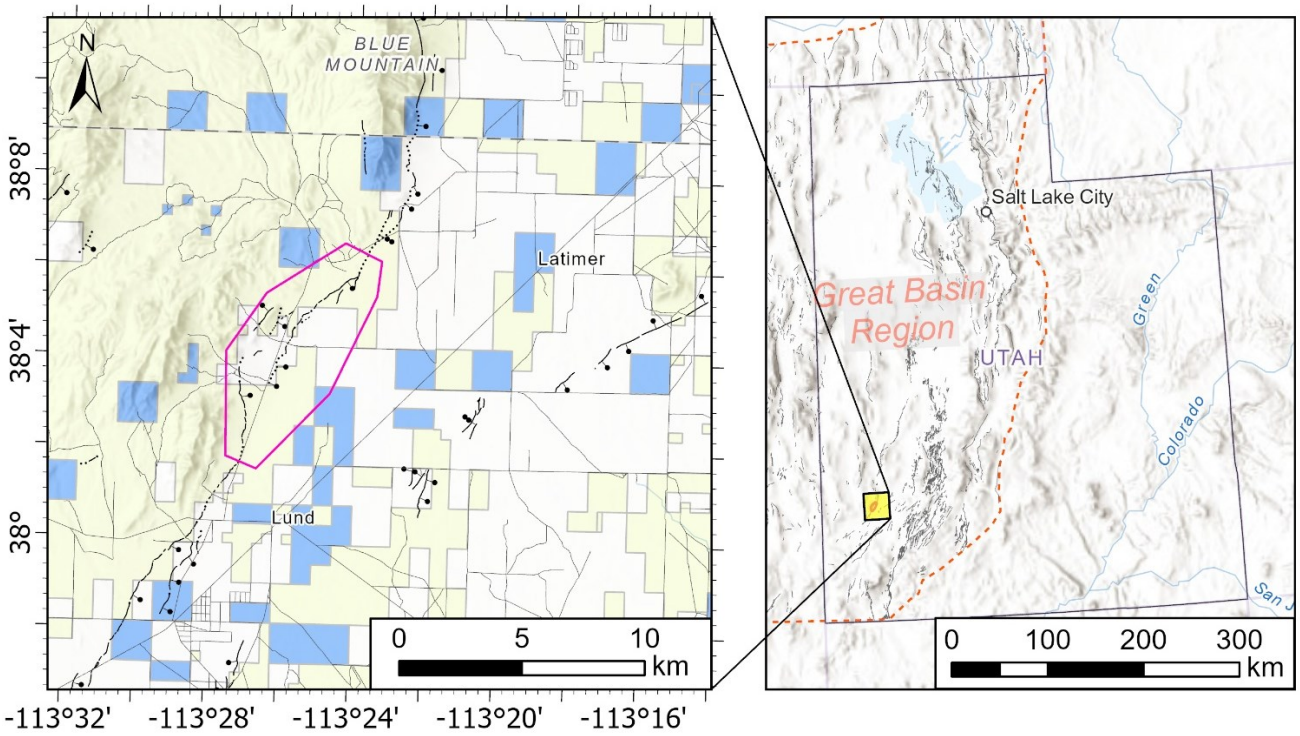

Figure 1: Left panel: The magenta polygon shows the general extent of the Lund North geothermal resource lead in Iron County, Utah, overlaid on a land ownership map containing private plots (white/blank), Bureau of Land Management (BLM) land (light yellow), and Utah Trust Lands (blue). Quaternary faults are shown as black lines with bar-balls indicating dip direction and local roads as light grey lines. Right panel: Quaternary fault traces (grey lines) and the eastern boundary of the INGENIOUS study area indicated by the dashed orange line. Land ownership from UGRC, 2024 and shaded basemap with regional labels from Esri, 2024.

As currently mapped, Lund North is a complex fault-bend and stepover structure centered near 38.44° N, -113.26° W that lies astride a large portion of private land in Iron County, Utah, with U.S. Bureau of Land Management land and Utah State Trust Lands around the perimeter. Local private landowners and lease holders were engaged to ensure successful site access and build a strong working relationship with Iron County residents. In exchange for transparent communication about planned fieldwork and advanced updates about technical results, the landowners and lease holders granted INGENIOUS partners full access to their land.

The detailed study of Lund North includes the compilation of the best available geological mapping, collection of samples to determine rock properties, detailed analyses of Quaternary faults, detailed geophysical surveys, geochemical analyses, a shallow temperature survey, and interpretation of a seismic reflection profile. Plans are to integrate results of these analyses into a 3D geological model, local-scale PFA, conceptual model, and resource assessment, which will be tested through thermal gradient well drilling. Here we present the current progress of the Lund North study site.

2. METHODS AND DATA

2.1 Geologic and structural mapping

2.1.1 Geologic setting

Surface geologic mapping in this region was conducted most recently in the 1990s (Grant et al., 1988; Hintze et al.,1994) and a set of GIS-based map products was published subsequently (Hintze et al., 2017). The scale of these maps is conducive to local geothermal resource assessment and, though no new geologic maps were produced for this study, several map elements (e.g., Quaternary faults) were updated to improve our understanding of the area (*refer to* section 2.1.2).

The geology of the Lund North area is characterized by typical Basin and Range geography that includes uplift horst blocks of bedrock adjoining broad intervening basins filled with a spectrum of unconsolidated and consolidated sedimentary and volcanic basin fill. The bedrock exposed in the upland areas adjoining the Lund North prospect includes a series of folded and faulted Mesozoic clastic sedimentary rocks structurally overlain by early Paleozoic carbonates and shales (Grant et al., 1988). Synorogenic conglomerates, related to slip and quiescence of eastward directed shortening of the Sevier fold and thrust belt, discontinuously overly the Paleozoic and Mesozoic rocks. These sections are overlain by sequences of Oligocene thru Miocene effusive volcanic rocks. In the Lund North area, the Oligocene-age rocks are characterized by thick contiguous packages of welded tuffs and minor intermediate composition lava flows sourced from the Caliente Caldera system to the west in Nevada (Best et al., 2013). Miocene-age rocks include felsic and mafic flows related to bimodal volcanism typical of the Basin and Range province (Hintze et al., 1994). All bedrock units are uplifted and separated from the adjoining basin to the east by a series of down-to-the-east normal faults related to ongoing Miocene through recent Basin and Range extension. Basin fill includes suites of surficial unconsolidated deposits that range from alluvial to eolian and lacustrine deposits. Older basin fill, locally exposed and throughout the basins at depth, includes similar facies with increasing lithification with depth. Locally the basin fill also contains basalt and felsic flows of spatially limited extent.

2.1.2 UAV lidar data and Quaternary fault mapping

In May 2024, approximately 10.15 km^2 (3.9 mi^2) of lidar data in the vicinity of the Lund North INGENIOUS research site were collected. A DJI Matrice M300 RTK uncrewed aerial vehicle (UAV) with a DJI Zenmuse L1 lidar scanner was used for data collection. For real-time kinematic (RTK) Global Navigation Satellite System (GNSS) corrections, a cellular data connection was used to receive corrections from The Utah Reference Network (TURN) GNSS base system. The data were collected in the field over the course of one week, with an additional day of office processing time. A resulting digital elevation model (DEM) with 0.22 m/pixel resolution allowed for highly detailed (1:2,500 scale or better) mapping of Quaternary-age fault scarps (Figure 2).

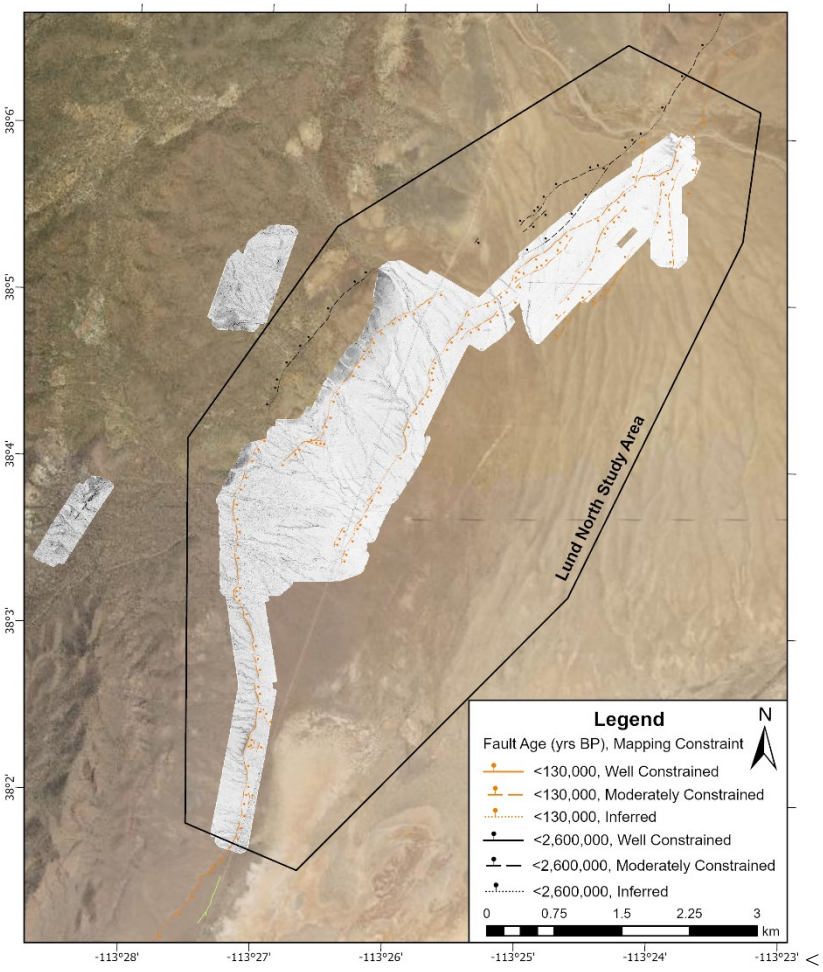

Figure 2. Map of the Lund North study area (black polygon). New UAV lidar shown as slopeshade (shaded by slope angle from 0-45 degrees) DEM image with new fault trace mapping shown as orange lines, dotted where inferred (bar-balls indicate fault dip direction). Basemap from Hexagon Imagery, 2024.

The fault crossing the Lund North site is called the Wah Wah Mountains (south end near Lund) fault in the Utah Quaternary Fault and Fold Database (Utah Geological Survey, 2024) or the Lund fault (Hintze et al., 2017). This fault runs approximately 37 km along the southern margin of the Wah Wah Mountains, cutting Late-Pleistocene-age alluvial fans. Previously, 1-m resolution, U.S. Geological Survey (USGS) Quality Level 2 lidar data (UGRC, 2020) was used for the initial Quaternary fault mapping at the Lund North site (Figure 3).

The range-front–alluvial-fan interface was the targeted area for collecting the UAV lidar data, due to most of the Quaternary-age faulting occurring on alluvial fans at the site (Hintze et al., 2017). This new lidar data allowed Quaternary-age fault scarps to be mapped in much greater detail than previously mapped. In many places, newly identified fault traces were mapped, adding to the detail and understanding of overall complexity of the fault zone. Many small fault step-overs (example in Figure 3), small zones of distributed faulting, and multiple small fault scarps were mapped using the high-resolution DEMs. Additionally, two small areas closer to the bedrock exposed at the site were targeted with the UAV lidar data collection for more detailed structural mapping (small, isolated areas in Figure 2). Overall, the UAV lidar data greatly aided new fault mapping, which expanded the complexity and length of the fault zone at the Lund North site.

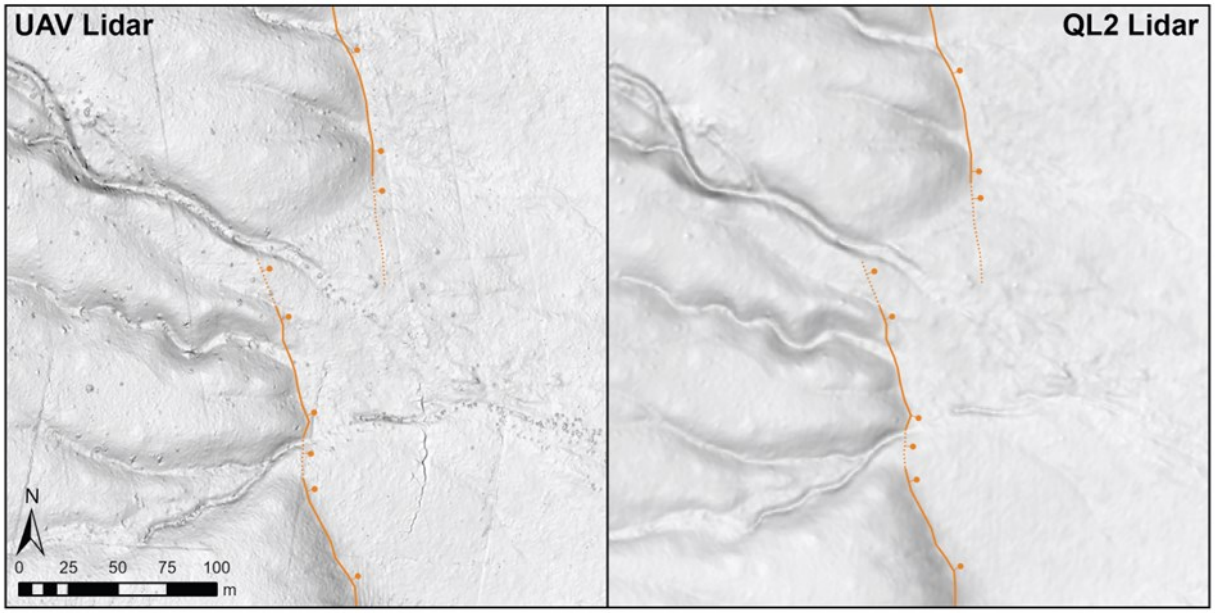

Figure 3. Comparison of 0.22 m/pixel resolution DEM from UAV lidar (left) and 1-m resolution DEM from airborne QL2 lidar (right); both shown as slopeshade images. Mapped fault traces shown as orange lines, dotted where inferred (bar-balls indicate fault dip direction). Straight, parallel lineaments visible on the left image (UAV lidar) are a processing artifact that we were unable to correct.

2.1.3 Outcrop Analysis

To complement and inform geophysical work, the Utah Geological Survey (UGS) collected a variety of rock samples from outcrops in the Lund North area to characterize bedrock petrology, bulk density, and reconnaissance magnetic susceptibility. Seventeen samples were collected from a range of geologic strata (Table 1).

Table 1: List of rock samples from outcrops. A variety of rock samples were collected from outcrops both in and around Lund North. Sampling was conducted to begin characterizing bedrock petrology ahead of geophysical work in the area.

Sample ID	Longitude	Latitude	Lithology	Unit Label	Geologic Unit
24LN-01	-113.467687	38.025202	tuff	Tw	Wah Wah Springs Fm
24LN-02	-113.469715	38.033186	tuff	Tl	Lund Formation
24LN-03	-113.465807	38.02383	tuff	Tel	Escalante Desert Formation
24LN-04	-113.469972	38.051644	tuff	Tl	Lund Formation
24LN-05	-113.463779	38.056616	tuff	Tw	Wah Wah Springs Fm
24LN-06	-113.469737	38.073082	dolostone	Cs	Swasey Limestone
24LN-07	-113.469822	38.072288	shale	Cw	Whirlwind Formation

24LN-08	-113.450191	38.080537	tuff	Ti	Isom Formation
24LN-09	-113.4441256	38.08207941	tuff	Ti	Isom Formation
24LN-10	-113.44439	38.08454286	tuff	Tbt	Blawn Formation
24LN-11	-113.443792	38.077853	sandstone	Jn	Navajo Sandstone
24LN-12	-113.43999	38.075855	conglomerate	Tcl	Claron (?) Formation
24LN-13	-113.423328	38.115111	tuff	Tcb	Condor Canyon Formation
24LN-14	-113.425481	38.130057	tuff	Tbt	Blawn Formation
24LN-15	-113.440044	38.159063	sandstone	Ts	sandstone and conglomerate
24LN-16	-113.381813	38.126121	basalt	Tsb	Steamboat Mountain Formation
24LN-17	-113.457980	38.064800	sandstone	Jn	Navajo Sandstone

2.2 Shallow (2 m) temperature survey

Shallow temperature surveys have been used in the Great Basin region to identify and map shallow thermal anomalies for over 40 years (Kraal et al., 2024, and references therein). An identified shallow thermal anomaly indicates elevated subsurface thermal gradients and can provide valuable insights into the extent and characteristics of geothermal systems, which is especially useful in exploration for hidden geothermal systems.

An initial reconnaissance 2-m survey was planned and conducted in November 2024, following the best practices outlined by Kraal et al. (2024). A total of 35 stations were collected in two days within the roughly 33 km^2 Lund North area of interest, mostly alongside existing dirt roads. The station spacing ranged from about 250 m to 1,000 m. The higher resolution spacing was implemented along Blue Mountain Road, between the intersections with the roads to Paramore Spring and Marsden Spring, as well as along those roads. This area was the main focus of the survey as it was inferred to be one of the most structurally complex parts of the Lund North study area and also near the location of the historical high heat flow measurement (Rush, 1983). Lower resolution spacing was applied progressively farther from this area.

The measured 2-m temperatures ranged from 15.7˚ to 19.1˚C with an estimated background temperature of 17.6˚C. Additional corrections were applied to the data to correct for effects due to albedo and elevation (see Kraal et al., 2024). The albedo correction was calculated using ASTER 07XT satellite images (DOI: 10.5067/ASTER/AST_07XT.003), and VNIR band 1 was used as it had the highest correlation with the 2-m temperature data. The elevation correction from LeSchack and Lewis (1983) was utilized with an elevation datum of 1,600 m. The albedo and elevation corrected 2-m temperature data ranged from 16.3˚ to 18.8˚C with an estimated background temperature of 17.8˚C. Degrees above background were calculated and are mapped in Figure 4.

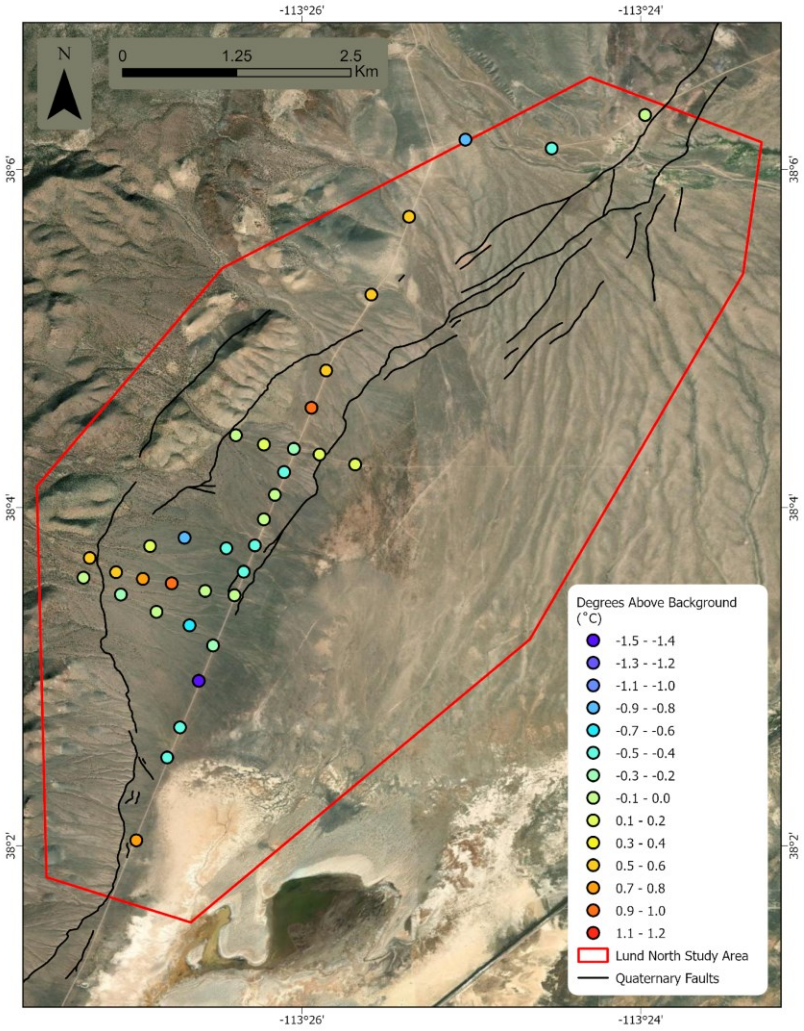

Figure 4: Colored points indicate albedo and elevation corrected 2-m temperatures mapped as degrees above background (˚C). The red polygon indicates the outline of the Lund North study area. Quaternary faults mapped from UAV-based lidar are represented by black lines. Basemap imagery from Esri, 2024.

2.3 Geochemistry

Fluid geochemistry, isotopic, and dissolved gas composition can provide basic constraints on the presence and character of blind geothermal systems, crustal-scale heat, and permeability (Simmons and Kirby, 2024). Groundwater from springs and existing wells is commonly sampled near areas of interest during the prospect phase of geothermal resource assessment. These data can help guide further exploration and confirm the presence of geothermal conditions at depth. Because of a lack of wells and limited natural springs in and near the Lund North prospect, a total of three samples were collected in September 2024. Two samples were taken from Paramore and Marsden Springs, and one sample was collected from a groundwater well southeast of the prospect near Lund (Figure 5). Field parameters measured during sampling included temperature (16.8˚–20.7˚C), pH (6.91–7.50), specific conductivity (674–1,059 µS/cm), and alkalinity (188–280 mg/L as $CaCO_3$). Water samples are currently being analyzed for major ion, select trace constituents, and stable isotopes of deuterium, oxygen-18, and carbon 13. These data will provide preliminary constraints on the near surface geochemistry and any potential evidence of thermal fluids at depth.

Based on preliminary results and previous regional groundwater investigations (Mower and Sandberg, 1982), the groundwater in the Lund North area has major ion composition that ranges from calcium-bicarbonate to sodium-chlorides or sodium-sulfates. These chemistries represent a continuum of geochemical evolution that is typical of Basin and Range groundwater systems where dilute bicarbonate-dominated waters typical of upland areas of recharge grade into more concentrated sodium-chloride waters in areas of discharge (Kirby et al., 2014). Total silica content is less than 10 ppm across all samples. A range of simple geothermometer calculations yielded potential equilibration temperatures below 40˚C. Stable isotopes of deuterium and oxygen-18 from these samples plot along the meteoric water line and show limited evidence of equilibration at high temperatures. Taken together, these data show little evidence of deep-seated geothermal fluids in this small sample set.

Figure 5: Water sample locations near the Lund North study area (red outline). Basemap imagery from Esri, 2024.

2.4 Geophysics

2.4.1 Seismic data

Licensing was acquired for a ~20-km-long segment of a two-dimensional (2D) seismic reflection data line (labeled "FC-3"; Figure 6) that extends from the heart of the Lund North study area into the Escalante Desert. Line FC-3 is 24 channel, 12 fold data that was shot by VIBROSEIS in 1969 and reprocessed in 2016 (data acquired from Seismic Exchange Inc., 2024). Although the legacy 2D seismic data in this region are of moderate quality overall, line FC-3 was purchased because of good data quality and its bifurcation of the Lund North site; these data have the potential to characterize the geometry, extent, and frequency of "basin-bounding" Quaternary faults. Key features in FC-3 data include high-amplitude, low-frequency, and laterally discontinuous reflector packages at relatively shallow depths and some deeper signals of mixed signal quality and range. These signals are notionally interpreted as being alluvial basin fill and mixed Cenozoic volcanic packages overtop Paleozoic-Mesozoic strata packages and potentially top of acoustic basement reflectors. Quaternary faults could be producing the sharp lateral discontinuities we observed—they lie in geologically realistic locations. Once integrated with planned potential field surveys that strategically overlie the trace of seismic data, line FC-3 will allow confident subsurface structural interpretation and relative stratigraphic interpretation.

2.4.2 Gravity

A total of 263 new gravity stations from this study were added to 109 stations from previous geothermal research related to Thermo Hot Springs (Hardwick, 2013). These 372 modern gravity stations will be combined with legacy gravity stations from INGENIOUS Phase 1 (Glen et al., 2022) to achieve better coverage in and around Lund North study area in the northern Escalante Desert (Figure 6). The spacing of newly acquired stations ranges from 100 to 500 m on detailed transects and approximately 1 km for fill-in of other areas. Field measurements were made using two Scintrex CG-5 gravimeters following the methods of Gettings et al. (2008); we used a 10-minute

time series with reoccupations of local and regional bases. Elevation control on most of the stations is better than 0.1 m, which was achieved through post-processing of high-precision, multiband GNSS data, resulting in a gravity accuracy of better than 0.03 mGal. Processing of field data is underway and preliminary outputs indicate that it is of high quality.

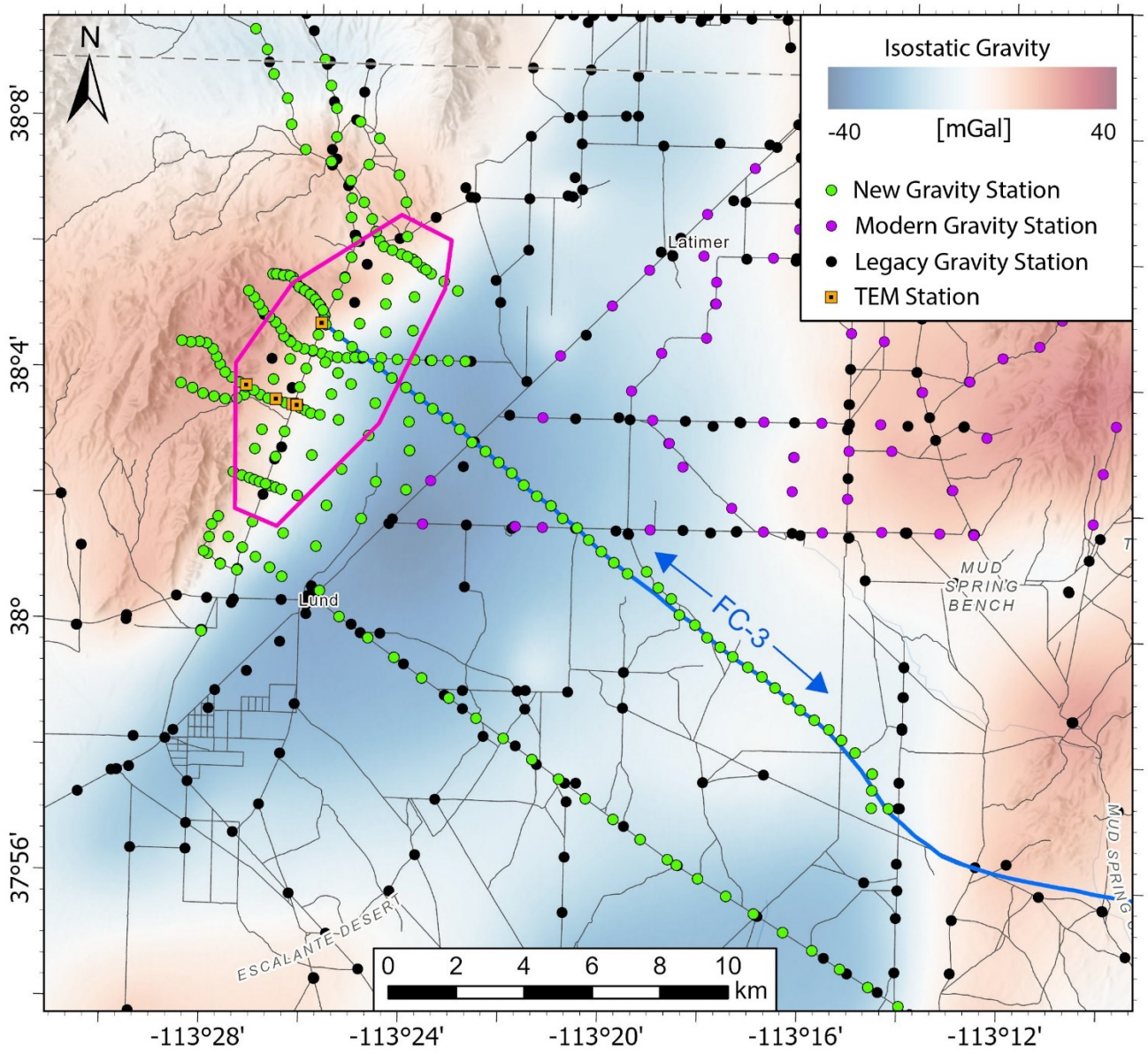

Figure 6. Map showing gravity stations for the study area and the isostatic gravity field from INGENIOUS Phase 1. Thin grey lines are local roads, magenta polygon is the Lund North FSS, and blue line is seismic section FC-3. Isostatic gravity gives a first order approximation of contrast between signals of local basins adjacent to mountain blocks (low vs. high density material). Road layer from UGRC, 2020 and shaded basemap with regional labels from Esri, 2024.

2.4.3 Magnetics

Two airborne magnetic and radiometric surveys (Figure 7) are currently being flown over southwest and central Utah as part of the USGS's Earth Mapping Resources Initiative (Earth MRI). Together these surveys cover the entire Lund North site and will provide high resolution magnetic data useful for constraining basin structure and locations of potential subsurface hydrothermal alteration. The survey specifications include a nominal flight height of 100 m with a line spacing of 200 m. Some of the data collection is complete whereas survey leveling and QA/QC is ongoing with final data expected in early 2025.

To augment aeromagnetic data, we collected oriented paleomagnetic cores at seven sites throughout the field area comprising 49 individual samples. Samples were collected with a gas-powered, water-cooled rock drill and oriented using a magnetic compass in a Pomeroy orienter. Samples are currently undergoing analysis at the Utah Paleomagnetic Center at the University of Utah and will constrain the remnant magnetization of geologic units at the Lund North site. Samples will be stepwise demagnetized in an alternating magnetic field and measured with an AGICO JR-6 spinner magnetometer. Additionally, we collected 22 hand samples from the exposed geology to constrain their physical rock properties. Density and magnetic susceptibilities obtained from these samples will be combined with the paleomagnetic data to serve as primary constraints for 2D and 3D geophysical models of the site.

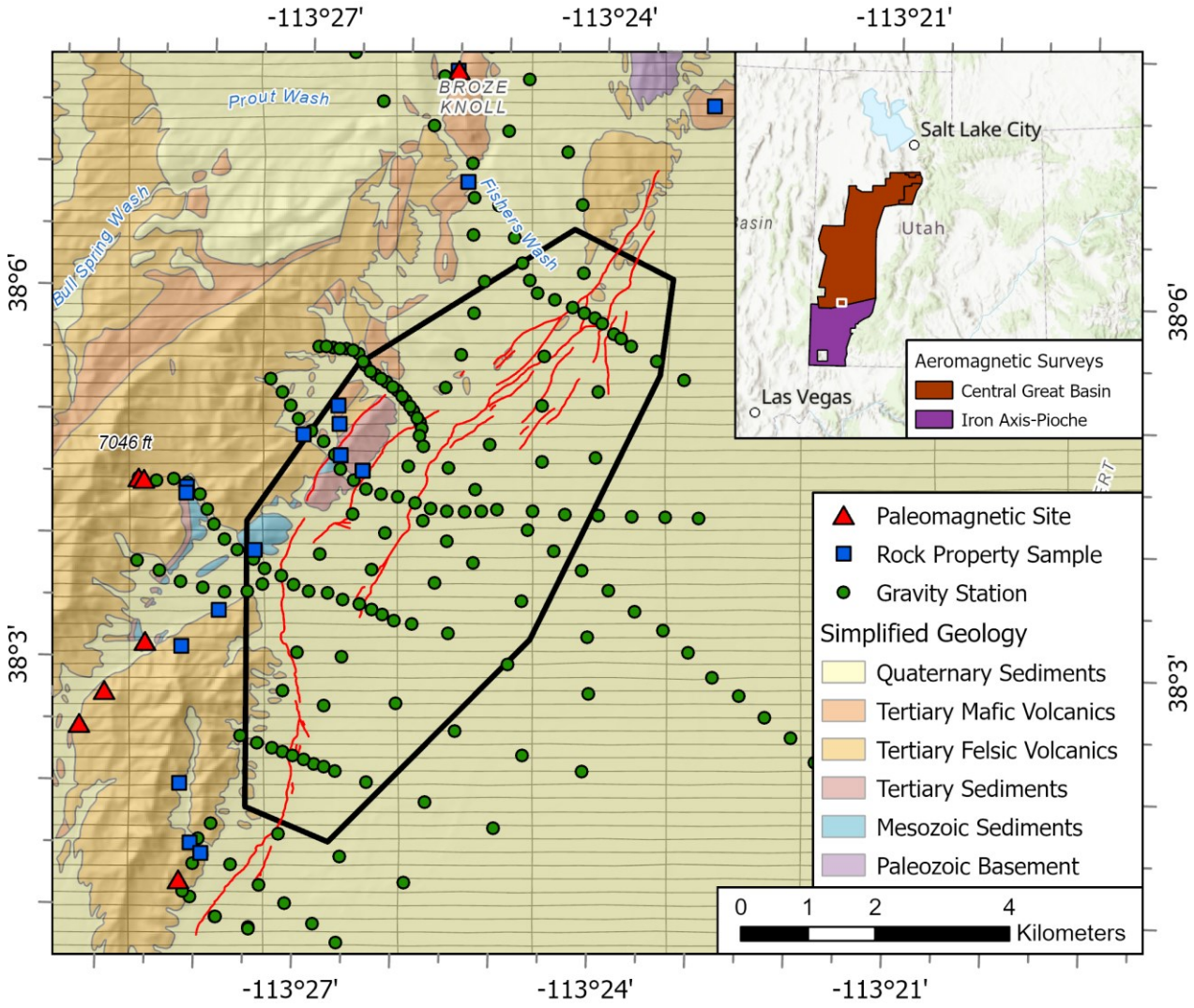

Figure 7: Map of the Lund North field site showing the simplified geology with the collected paleomagnetic and rock property sampling sites along with the gravity station locations. Grey lines indicate the flight lines for the two aeromagnetic and radiometric surveys (full survey extents shown on inset map). Updated Quaternary faults shown in red. Base map from the ArcGIS online map server (Esri, 2024).

2.4.4 Magnetotellurics (MT)

Magnetotellurics (MT) is a passive electromagnetic measurement meaning no energy is put into the ground: the instruments only listen to natural electric and magnetic signals. By measuring these signals, information about the electrical resistivity structure of the subsurface can be estimated. MT is directly sensitive to where fluids are or have been in the subsurface, making it ideal for characterizing geothermal systems. MT data were collected on a grid with nominal site spacing of 2 km (52 stations) in May 2024 (Figure 8). MT data were recorded using 32-bit Zen receivers developed by Zonge International. Magnetic fields were recorded for both horizontal directions (geomagnetic north and east) and the vertical direction using ANT-4 induction coils. Electric fields were recorded for geomagnetic east and north using Ag-AgCl reference electrodes with dipole lengths around 50 m depending on topography. Data were recorded at two different sample rates. For 7 hours and 50 minutes, data were recorded at 256 samples/s, then changed to 4,096 samples/s for 10 minutes. This couplet was then repeated for at least 20 hours. Data loggers were programmed such that all instruments recorded the same schedule for remote reference processing.

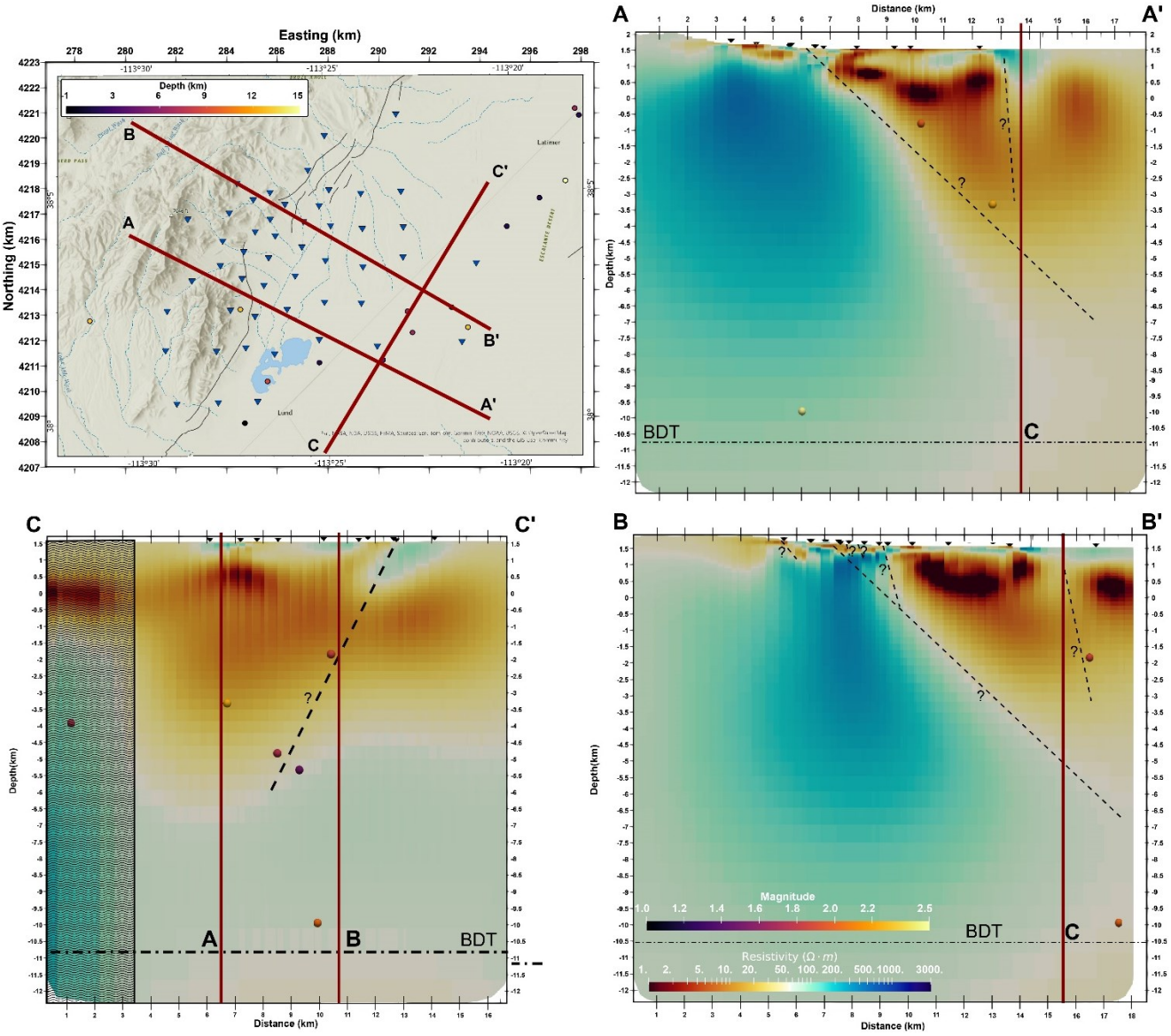

Figure 8. Profiles from the 3D electrical resistivity model as shown on the MT station (blue triangles) map in the upper left, coordinate system reference is NAD 83 UTM zone 12N. Orange star: warm spring; dashed lines: inferred faults. Earthquake hypocenters shown are from the ANSS Earthquake catalog (U.S. Geological Survey, 2017). Base map in figure 8A is from the ArcGIS online map server (Esri, 2024).

MT transfer functions were estimated using an open-source Python workflow. Time series data were input into an MTH5 (Peacock et al., 2022) for each station including a time series of all runs combined and down sampled to 1 sample/s. The processing code Aurora was used to estimate MT transfer functions (Kappler et al., 2024). Synchronous stations were used as remote references and for periods longer than 4 seconds magnetic observatory data from Fresno, California, were used. Data are generally good from periods 0.001 to 5,000 seconds, with some data good to 8,000 seconds due to a strong geomagnetic storm (see Figure 9). Final transfer functions were rotated to geographic north using MTpy-v2 (Kirkby et al., 2019).

A 3D electrical resistivity model was developed using the inversion software ModEM (Kelbert et al., 2014). Input files were created using MTpy-v2, which includes the data file and model file. MT data inverted include 23 periods spaced logarithmically between 0.002 to 3,000 seconds. Both the impedance tensors and induction vectors were inverted for using an error of 3% of the Eigen values of the impedance tensor and an absolute error floor of 0.02 for the induction vectors. The model grid is 83 x 90 x 115 cells (300 km x 300 km x 300 km) where horizontal cell dimensions within the station area are 200 x 200 m with increasing size outside the station area by a factor of 1.5. Vertical cells start at a thickness of 23 m and increase geometrically by a factor of 1.2 below mean surface level. Above mean surface level to the top of maximum topography the cell thickness is constant at 23 m to include topography in the model. A preliminary model was developed using a 50 Ohm-m half-space as the starting model, including topography. The covariance was set to 0.2 in all directions and applied twice. Starting lambda was set to 100. The model ran for 109 iterations and reduced the misfit from 46 to 4.8.

The preliminary 3D electrical resistivity model provides important insights into the subsurface of the study area (Figure 8). In this part of the GBR, low resistivities (<60 Ohm-m) tend to be characteristic of basin-fill materials, whereas high resistivities are more indicative of bedrock lithologies (all other factors being equal). Shapes and geometries observed in the resistivity model could be interpreted as structures at first glance assuming there is background knowledge of the area. One such inference from the resistivity model is that the dominant structure is a large, east-dipping normal fault consistent with other datasets in the study area. To the west of this inferred fault, electrically conductive anomalies about 500 m thick occur near known springs, possibly related to fluids and circulation. Additionally, no deep conductive anomaly is observed in the model within the study area. The brittle-ductile transition is around 11 km, where there is a possible breach in the southeast of the study area suggesting fluids and/or heat penetrates the crust as indicated by earthquake hypocenters and low resistivity. Further investigation in careful detail could support the development of a robust conceptual model.

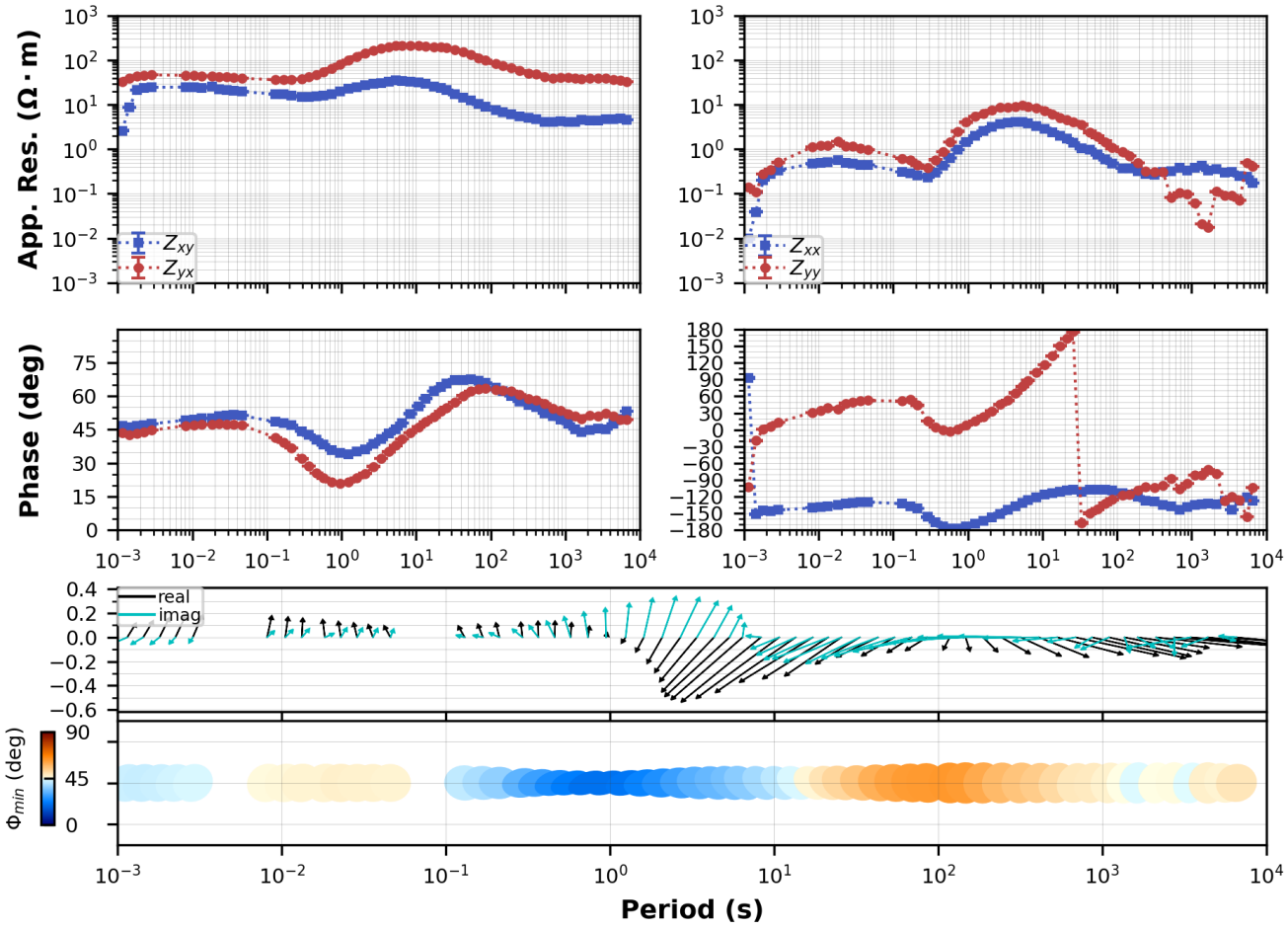

Figure 9: Example of an MT response for Lund North MT station ld142. These data were collected during the geomagnetic storm showing good data down to 8,000 seconds with just 18 hours of recorded data. Apparent resistivity and phase are the top two rows, respectively, showing various components of the impedance tensor. Induction vectors are in the third row indicating a strong lateral boundary at around 1 s period. Phase tensors are in the bottom row colored by the minimum phase, which shows a strong resistivity change at around 1 s period.

2.4.5 Transient electromagnetic (TEM) survey

We conducted TEM geophysical survey tests to better define subsurface structures and features near the study site and supplement MT resistivity models in the shallow subsurface. TEM is an active-source method that measures the attenuation signal of induced magnetic fields corresponding to changes in the electrical properties in the subsurface. TEM test measurements were made at five unique locations within the study area (Figure 6) using an ABEM WalkTEM ground loop system fitted with a 40- x 40-m transmitter antenna as well as high- and low-frequency receiver antenna coils capable of simultaneous recording. The time spent at each station location was around one hour with two to three measurements completed during that time as well as subsequent checking of the field data. All TEM stations yielded high-quality data with good signal-to-noise ratios.

After initial data processing, preliminary one-dimensional (1D) inversion models for every station were created (Auken et al., 2015) and improved by screening data bands until data fit was satisfactory. 1D resistivity models are constrained using the depth of investigation (DOI) parameter (refer to Spies, 1989; Christiansen and Auken, 2012). DOI is unique for each station, relies on the physical properties of subsurface material, and indicates the maximum depth of resolution with respect to modeling. When extending modeling deeper than the DOI, confidence in the resulting 1D and 2D models will subsequently decrease with increasing depth.

The DOI values for the study area range from approximately 200 m to 400 m with an average of 300 m. Background resistivity values within the study area range from 10 to 300 Ohm·m, which are inferred to be the signature of fine, clay-rich valley fill (low resistivity, approximately 10 to 30 Ohm·m) as well as coarser fill on the alluvial fans consisting of sand, gravel, and volcanics that are closer to their sources (high resistivity, 100–1,000 Ohm·m).

3. NEXT STEPS

3.1 Geologic and structural mapping

High-quality geologic mapping exists at a 1:50,000 scale across the study area (Hintze et al., 2017), which is sufficient for site characterization and the creation of derivative map products. Some individual map elements, such as Quaternary fault traces, have been updated as part of this study (*refer to* Section 2.1.2.) but no new geologic mapping is planned.

3.2 Shallow (2 m) temperature survey

At this time, the preliminary results are being interpreted to determine if additional data collection is necessary.

3.3 Geochemistry

Once analyses for major ion, select trace constituents, and stable isotopes of deuterium, oxygen-18, and carbon-13 are complete, the results can be used to calculate conventional geothermometers as well as multicomponent equilibrium geothermometry estimates.

3.4 Geophysics

Processing of all geophysical field data will be completed. Gravity and magnetic data can be used in conjunction with the rock property data to construct a series of geophysical 2D forward models. Combined with the MT electrical resistivity model, shallow TEM resistivity models, and seismic line interpretations, these data can serve as inputs for 3D models of the Lund North site. These models can help identify the most favorable locations for thermal gradient well drilling.

3.5 Modeling

The data collected above can be integrated to develop 3D geological, geophysical, and geostatistical models, as well as conceptual resource models that incorporate hydrogeological components (e.g., Ayling and Hinz, 2020). Additionally, PFA can be applied to produce local-scale geothermal favorability maps (e.g., Faulds et al., 2019). These conceptual and geostatistical models can then be utilized to apply power density approaches (e.g., Cumming, 2016) to quantitatively estimate geothermal resource potential with associated uncertainties (P10, P50, P90) at the Lund North study site. A combination of these products, especially the conceptual resource modeling results and hypotheses about resource geometry/temperature can be utilized to identify optimal locations of thermal gradient holes to test the models of this site. These thermal gradient wells can provide information on the subsurface thermal profile, lithologies, structure, mineralogical characteristics of subsurface formations, and possibly water chemistry. These new subsurface datasets can then be used to update the conceptual model of the Lund North site and revise resource estimates as needed.

4. ACKNOWLEDGEMENTS

This project is funded by the United States Department of Energy—Geothermal Technologies Office under award DE-EE0009254 to the University of Nevada, Reno. Any use of trade, firm, or product names is for descriptive purposes only and does not imply endorsement by the U.S. Government. We thank the Utah Trust Lands Administration and Cedar City BLM Field Office staff for working with us in an efficient and timely manner enabling us to complete these field surveys. We would also like to thank Ian Adams and Nada Mareechi Jacinto for their assistance in completing the 2-m temperature survey presented in this paper.

REFERENCES

Ayling, B., Faulds, J.E., Clark, A., Morales-Rivera, A., Sladek, C., Berti, C., Kreemer, C., Siler, D., Mlawsky, E., Gentry, E., Kleber, E., Burns, E., Warren, I., Batir, J., DeAngelo, J., Peacock, J., Witter, J., Queen, J., Glen, J.M.G., Kraal, K., Mann, M., Wagoner, N., Williams, N., Dobson, P., Micander, R., Koehler, R., Kirby, S., Brown, S., Earney, T.E., Cladouhos, T., Rickard, B., Trainor-Guitton,

W., Lifton, Z. "INnovative Geothermal Exploration through Novel Investigations Of Undiscovered Systems (INGENIOUS) Project Introduction and Activity Update." Proceedings: GRC Transactions, 46, (2022).

Ayling, B. F., & Hinz, N. H.: Developing a conceptual model and power capacity estimates for a low-temperature geothermal prospect with two chemically and thermally distinct reservoir compartments, Hawthorne, Nevada, USA: Geothermics, 87, 101870 (2020).

Auken, E., Christiansen, A.V., Kirkegaard, C., Fiandaca, G., Schamper, C., Behroozmad, A.A., Binley, A., Nielsen, E., Efferso, F., Christensen, N.B., Sorensen, K., Foged, N., and Vignoli, G.: An overview of a highly versatile forward and stable inverse algorithm for airborne, ground-based and borehole electromagnetic and electric data: Exploration Geophysics, v. 46, (2015), p. 223–235.

Christiansen, A.V., and Auken, E.: A global measure for depth of investigation: Geophysics, v. 77, no. 4, (2012), p. WB171– WB177.

Best, M.G., Christiansen, E.H., Deino, A.L., Gromme, S., Hart, G.L., and Tingey, D.G.: The 36–18 Ma Indian Peak–Caliente ignimbrite field and calderas, southeastern Great Basin, USA: Multicyclic super-eruptions. Geosphere; 9 (4), (2013): 864–950. https://doi.org/10.1130/GES00902.1

Cumming, W.: Resource capacity estimation using lognormal power density from producing fields and area from resource conceptual models; advantages, pitfalls and remedies. Proceedings, 41st Workshop on Geothermal Reservoir Engineering, Stanford University, Stanford, CA (2016), 7 p.

Faulds, J., and Hinz, N.: Favorable tectonic and structural settings of geothermal systems in the Great Basin region, western USA: Proxies for discovering blind geothermal systems, Proceedings World Geothermal Congress, Melbourne, Australia (2015) https://www.osti.gov/biblio/1724082

Faulds, J.E., Hinz, N.H., Coolbaugh, M.F., Ramelli, A., Glen, J.M, Ayling, B.A., Wannamaker, P.E., DeOreo, S.B., Siler, D.L., and Craig, J.W.: Vectoring into potential blind geothermal systems in the Granite Springs Valley area, western Nevada: Application of the play fairway analysis at multiple scales: Proceedings 44th Workshop on Geothermal Reservoir Engineering, Stanford University, Stanford, CA, SGPTR-214, (2019), p. 74-84

Gettings, P., Chapman, D.S., and Allis, R.: Techniques, analysis, and noise in a Salt Lake Valley 4D Gravity experiment: Geophysics, v. 73, no. 6, (2008), p. WA71–WA82.

Glen, J.M., Earney, T.E., Zielinski, L.A., Schermerhorn, W.D., Dean, B.J., and Hardwick, C.: Regional geophysical maps of the Great Basin, USA: U.S. Geological Survey data release, (2022), https://doi.org/10.5066/P9Z6SA1Z

Grant, K.S., Hintze, L.F., and Best, M.G., Geologic map of the Lund Quadrangle, Iron County, Utah. OFR-178. UGS. 1:24,000 scale. (1988) https://doi.org/10.34191/OFR-178

Hardwick, C.L.: Geothermal Resources in Southwestern Utah: Gravity and Magnetotelluric Investigations, University of Utah, M.S. thesis, (2013), 67 p.

Hart-Wagoner, N., Coolbaugh, M., Faulds, J.E., Mlawsky, E., Lindsey, C., and Trainor-Guitton, W.: Preliminary Regional Play Fairway Workflow for the Great Basin Region, USA. Proceedings, 49th Workshop on Geothermal Reservoir Engineering, Stanford University, Stanford, CA, SGP-TR-227, (2024).

Hintze, L.F., Grant, S.K., Weaver, C.L., and Best, M.G., Geologic map of the Blue Mountain-Lund area, Beaver and Iron Counties, Utah, Miscellaneous Investigation Series Map I-2361. UGS. 1:50,000 scale. (1994) https://doi.org/10.34191/M-156

Hintze, L.F., Grant, S.K., Weaver, C.L., and Best, M.G.: Geologic map of the Blue Mountain - Lund area, Beaver and Iron Counties, Utah (GIS reproduction of USGS Map I-2361 [1994]: Utah Geological Survey Open-File Report 678DM, 1:50,000 scale, (2017), 1 pl., https://doi.org/10.34191/OFR-678dm.

Kappler, K., Peacock, J., Egbert, G., Frassetto, A., Heagy, L., Kelbert, A., Keyson, L., Oldenburg, D., Ronan, T., and Sweet, J.: Aurora: An open-source Python implementation of the EMTF package for magnetotelluric data processing using MTH5 and mt_metadata. Journal of Open Source Software. 9. 6832, (2024), 10.21105/joss.06832.

Kelbert, A., Meqbel, N., Egbert, G., and Tandon, K.: ModEM: A modular system for inversion of electromagnetic geophysical data. Computers & Geosciences. 66. (2014), 40-53. 10.1016/j.cageo.2014.01.010.

Kirby, S.M., Wallace, J., and Lowe, M.: Hydrochemistry, Water Quality, Dissolved Gas, and Isotopic Data for Groundwater in the Snake Valley Area and Implications for Groundwater Flow Paths: in Hurlow, H., editor, Hydrogeologic Studies and Groundwater Monitoring in Snake Valley and Adjacent Hydrographic Areas, West-Central Utah and East-Central Nevada: Utah Geological Survey Bulletin 135, (2014), p. 126-195.

Kirkby, A.L., Zhang, F., Peacock, J., Hassan, R., and Duan, J.: The MTPy software package for magnetotelluric data analysis and visualisation. Journal of Open Source Software, 4(37), (2019), 1358. https://doi.org/10.21105/joss.01358

Kraal, K.O., Lindsey, C., Zimmerman, J., Sladek, C., and Burgess, Q.: Development of shallow (2-m) temperature survey standard operating procedures and interpretation workbook: Proceedings, 49th Workshop on Geothermal Reservoir Engineering, Stanford University, SGP-TR-227, (2024), 34 p.

LeSchack, L.A. & Lewis, J.E.: Geothermal prospecting with Shallo-Temp surveys. Geophysics, 48, 7, (1983), p. 975-996.

Mower, G.W., and Sandberg, R.W.: Hydrology of the Beryl-Enterprise Area, Escalante Desert, Utah, With an Emphasis on Groundwater: State of Utah Department of Natural Resources, Technical Publication no. 73, (1982), 11 plates, 66 p.

Peacock, J., Kappler, K., Heagy, L., Ronan, T., Kelberd, A., and Frassetto, A.: MTH5: An archive and exchangeable data format for magnetotelluric time series data, Computers and Geoscience, 162, 105102, (2022). https://doi.org/10.1016/j.cageo.2022.105102.

Rush, F.E.: Reconnaissance of the hydrothermal resources of Utah. U.S. Geological Survey Professional Paper, 1044-H, (1983).

Simmons, S. F., and Kirby, S.: Formation of a large cold groundwater mantle helium anomaly and high temperature geothermal resources in response to bimodal magmatism near Roosevelt Hot Springs and Utah FORGE, Milford Valley, southwest Utah. Geochemistry, Geophysics, Geosystems, 25, e2024GC011539, (2024). https://doi.org/10.1029/2024GC011539

Spies, B.: Depth of investigation in electromagnetic sounding methods: Geophysics, v. 54, no. 7, (1989), p. 872–888.

U.S. Department of Energy (DOE): GeoVision: Harnessing the Heat Beneath Our Feet. Washington D.C.: U.S. Department of Energy. DOE/EE-1306, (2019), www.energy.gov/eere/geothermal/geovision.

U.S. Geological Survey, Earthquake Hazards Program: Advanced National Seismic System (ANSS) Comprehensive Catalog of Earthquake Events and Products: Various, (2017), https://doi.org/10.5066/F7MS3QZH.

Utah Geospatial Reference Center (UGRC), 2020, 2020 Central and Southern Utah Lidar Data: https://gis.utah.gov/products/sgid/elevation/lidar/#2020-southern-utah, accessed May 2024. Utah Geological Survey, Utah Geologic Hazards Portal: https://hazards.geology.utah.gov/, accessed December 11, 2024

Williams, C.F., Reed, M.J., DeAngelo, J., and Galanis, S.P. Jr.: Quantifying the undiscovered geothermal resources of the United States: Geothermal Resources Council Transactions, v. 33, (2009), p. 995-1002.